CFD simulation of unstable fluid flows in the rotor of a high-speed precipitation centrifuge

Sergey Mordanov[1*], *Anatoly* Khomyakov[1], *Victoria* Gushshamova[1], *Elizaveta* Vlasova[1], *Mikhail* Beloded[2], and *Pavel* Shkurin[2]

[1]Ural federal university, Department of Machines and Apparatuses for Chemical and Nuclear Production, Ekaterinburg, Russia
[2]SverdNIIhimmash JSC, Ekaterinburg, Russia

Abstract. The results of a numerical study of unstable fluid flows in the rotor of a high-speed vertical precipitation centrifuge are presented. It is shown that during the operation of a high-speed precipitation centrifuge, a qualitative change in the hydrodynamic regime is possible from conditionally laminar to conditionally turbulent, characterized by large-scale axial and radial pulsations of the liquid phase, accompanied by a significant decrease in sedimentation efficiency. It has been established that the flow pulsations are not random in nature, but the amplitude of these pulsations first increases with increasing rotation rate of the centrifuge rotor, and after passing a certain "critical" rotation rate it begins to decrease. Thus, the "critical" rotor rotation rate can be considered as a resonant rate, at which the frequency of turbulent flow pulsations (natural oscillation frequency) coincides with the rotor rotation frequency (forced oscillation frequency). The dependences of the pitch, frequency, and amplitude of liquid flow pulsations on the edge of the centrifuge overflow disk on the rotor rotation rate were obtained. It has been established that in the "subcritical" and "supercritical" operating modes, the amplitude and step of liquid pulsations on the overflow disk of the centrifuge are increasing and decreasing respectively.

1 Introduction

Centrifuges are widely used in the chemical industry and related industries to separate heterogeneous systems with differences in component densities. Due to the influence of centrifugal force, separation of components occurs components with high density move from the centrifuge axis to the walls of the rotor, components with low density move to the center of the rotor. The centrifugal force acting on a particle in a centrifuge rotor and the gravity force of gravity precipitation settling can be calculated as:

$$C=m\Omega^2 r, \quad (1)$$

$$G=mg. \quad (2)$$

There C is a centrifugal force, N; m is a mass, kg; Ω is an angular velocity, rad/s; r is a radial coordinate, m; G is a gravity force, N; g is a gravity acceleration, m/s^2.

* Corresponding author: s.v.mordanov@urfu.ru

The dimensionless ratio of centrifugal force to gravity is called the centrifugal separation factor [1, 2]. The centrifugal separation factor is one of the main variables used in calculating centrifuges.

$$\Phi = \frac{C}{G} = \frac{\Omega^2 r}{g}. \quad (3)$$

There Φ is a centrifugal separation factor.

Other important variables that are used when calculating centrifuges for a solid-liquid phases separation include the dispersed composition of the solid phase, the concentration of the solid phase, the difference in the densities of the heavy and light phases, the viscosity of the liquid phase, solid particles precipitation surface, and other factors [1, 2].

As follows from equation (3), increasing the value of the centrifugal separation factor, and therefore the efficiency of the centrifuge, is possible both by increasing the diameter of the centrifuge rotor and by increasing the angular velocity of the rotor. Moreover, as the diameter of the centrifuge increases, the centrifugal separation factor increases linearly, and with an increase in the angular speed of the rotor, the centrifugal separation factor increases to the second power. Centrifuges with a centrifugal separation factor greater than 3500 are classified as high-speed.

Typically, the engineering calculation of a centrifuge comes down to determining the main dimensions of the rotor and stator, determining the required rotor speed, calculating the rotor support units, strength calculations, and vibration resistance calculations (especially for high-speed centrifuges) [1].

Engineering calculations for vibration resistance come down to calculating strength under conditions of cyclic loads during rotation of the centrifuge rotor and determining the natural vibration frequencies of the rotor body to eliminate unacceptable dynamic deflections under conditions of resonance of the rotor's own natural vibration frequency and the forced vibration frequency (rotor rotation frequency) [3-5].

Calculation of the stability of fluid flow (suspension) through the rotor is not usually performed in engineering calculations. Turbulent pulsations of flows in the rotor can be considered only as one of the risk factors for the possible occurrence of dynamic vibrations of the rotor body. The influence of turbulent pulsations of liquid flows in the rotor on the efficiency of sedimentation in a centrifuge is usually not considered during engineering calculations.

At the same time, the phenomena associated with the occurrence of instability in fluid flows in the field of centrifugal force are known and are an important subject of research in hydrodynamics. In particular, the works [6-9] is devoted to the phenomenon of instability of a liquid thin layer on a rotating surface.

Among the works that consider the instability of flows in conditions close to the centrifuge rotor, papers [10, 11] should be highlighted. Work [10] is devoted to the study of radial instability near the surface of a rotating cylinder of small radius placed in a cylindrical container of large radius filled with a sodium chloride solution at rotation frequencies of the internal cylinder up to 1.84 rad/s. The authors of work [10] present experimental velocity profiles on the cylinder surface and in the volume of the liquid and, based on the results of processing experimental data, present the dependences of the dimensionless time of onset of flow instabilities and wavelengths on the surface of the cylinder on the Reynolds criterion, calculated from the linear velocity on the surface of the rotating cylinder. Work [11] is devoted to the study of the instability of flows in a volume of liquid located between two cylindrical walls rotating at the same angular velocity. The authors of [11] provide experimental and calculated data on the shape and quantitative characteristics of periodic vortices arising in the volume of liquid, the dependence of the Taylor number on the dimensionless width of the gap (thickness of the liquid layer) between rotating cylinders. Also, work [11] proposes a procedure for the numerical calculation of unstable flows for a volume of liquid located between two rotating cylinders.

Thus, works [6-11] and other similar works can be useful for simulating the operation of centrifuges (especially for batch centrifuges).

Our work is devoted to CFD simulation of unstable liquid flows in the rotor of a high-speed semi-continuous action precipitation centrifuge (with periodic sludge discharge).

2 Experimental research and early numerical simulations

In our previous works [12, 13], we tested the adequacy of the numerical modeling technique for fluid hydrodynamics in the rotor of a vertical high-speed precipitation centrifuge with rotor diameter of 150 mm. The adequacy of the numerical calculation was assessed by comparing the duration of displacement of an aqueous solution of glycerol from the volume of the centrifuge using a solution of photo fixer. The experimental research and CFD simulations for works [12, 13] were carried out in parallel by two independent research groups from SverdNIIhimmash JSC (experimental research) and the Ural federal university (simulations).

Figure 1 shows a scheme of the experimental test-stand. The test-stand consist of the glycerin solution vessels 1, photo fixer vessel 2, feeding pump 3, centrifuge 4, centrate vessel 5, sampler 6, flowmeter F, and tachometer n. The test-stand works as follows. Before starting measurements, the required rotation speed of the centrifuge rotor was set, and the rotor was filled with a glycerol solution of 15% by mass. The rotation speed was measured by tachometer n. After filling the centrifuge rotor with glycerin solution, the feeding of the photo fixer solution was started. The photo fixer solution flow flow measured by flowmeter F. Centrate samples were taken using a sampler 6 every 2 minutes from the moment the photo fixer solution starts to be feed. The displacement of glycerin solution from the centrifuge rotor was assessed by changes in the glycerol content in centrate samples.

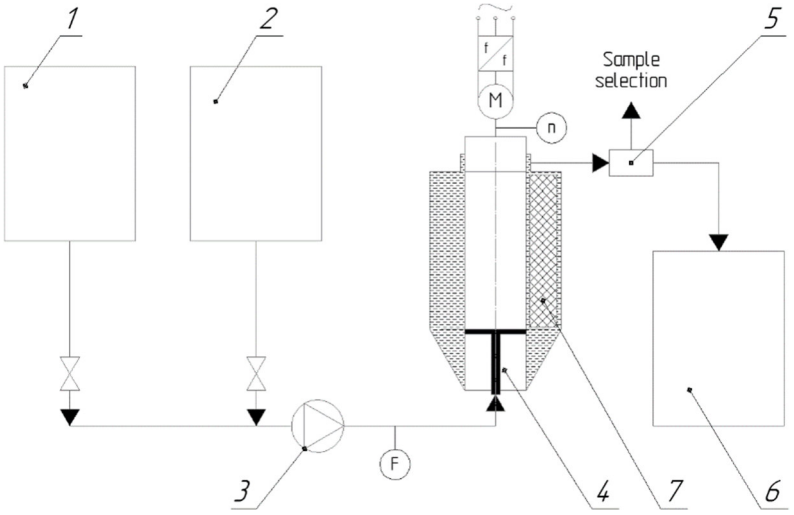

Fig. 1. The experimental test-stand scheme: 1 – glycerin solution vessels, 2 – photo fixer vessel, 3 – feeding pump, 4 – centrifuge, 5 – centrate vessel, 6 – sampler, F – flowmeter, n – tachometer, 7 – photographic film strip, M – centrifuge drive motor.

Experimental measurements were carried out for centrifuge rotor rotation speeds of 5,000, 6,500 and 8,000 rpm. The rotation speed of the centrifuge rotor was adjusted by changing the frequency of the electric current of the drive motor M. Measured density and viscosity of the glycerin solution for all experiments were 1.03 g/cm^3 and 219 cSt, respectively. Measured density and viscosity of the photo fixer solution for all experiments

were 1.0 g/cm^3 and 1.0 cSt, respectively. The flow of the photo fixer solution in all considered cases was maintained at 40 l/h.

In addition, in each experiment, a strip of photographic film 7 was installed in the centrifuge rotor. After the end of the experiment, the photographic film was developed and the hydrodynamics of the flows in the centrifuge rotor were obtained from the resulting photographic image.

In works [12, 13], for numerical CFD simulation, we used a mathematical model based on the Navier-Stokes equations in the multiphase Manninen's formulation [14], the standard k-epsilon turbulence model [15], the interaction of the rotor and stator using moving reference (MRF) [16], and 2D axisymmetric rectangular computational mesh with about 10^5 elements density (Figure 2). The simulation was carried out using ANSYS Fluent code using the pressure-based solver program and relative velocity formulations.

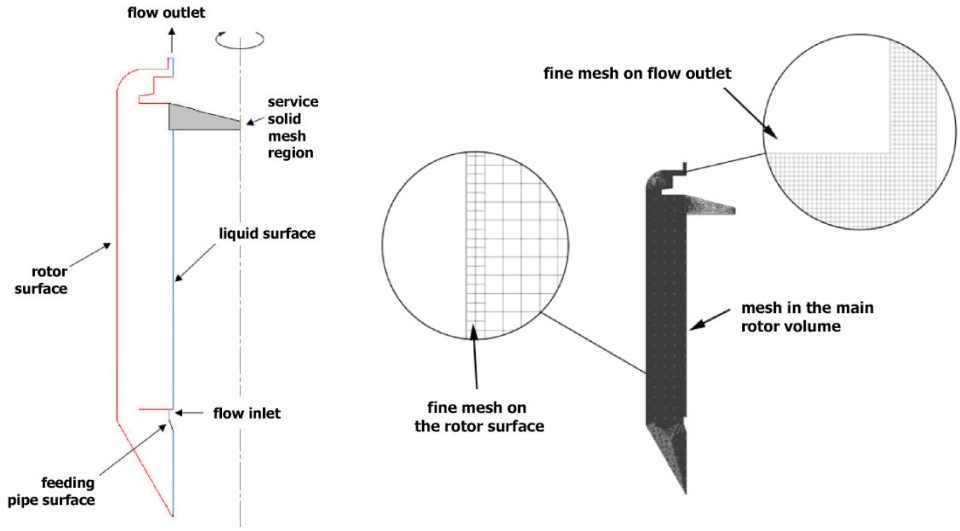

Fig. 2. 2D geometric model (a) and axisymmetric rectangular computational mesh (b).

In Manninen's formulation, the mass conservation equation for a model of a mixture of n components in the absence of additional sources of mass takes the form [14]:

$$\frac{\partial \rho_m}{\partial t} + \left(\frac{\partial \rho_m u_x}{\partial x} + \frac{\partial \rho_m u_y}{\partial y} + \frac{\partial \rho_m u_z}{\partial z}\right) = 0, \tag{4}$$

$$\boldsymbol{u_m} = \frac{\sum_{\varphi=1}^{n} \alpha_\varphi \rho_\varphi \boldsymbol{u_\varphi}}{\rho_m}, \tag{5}$$

$$\rho_m = \sum_{\varphi=1}^{n} \alpha_\varphi \rho_\varphi, \tag{6}$$

$$\sum_{\varphi=1}^{n} \alpha_\varphi = 1. \tag{7}$$

There m is a mixture properties index; φ is a phase (component) properties index; t is a time, s; u is a velocity, m/s; n is an phases (components) quantity; x, y, z are Cartesian coordinates, m; α is a phase (component) volume fraction; ρ is density, kg/m^3.

The momentum conservation equation along the Cartesian axis i for a mixture of components (phases) in Manninen's formulation in the absence of additional sources of momentum has the form [14]:

$$\frac{\partial}{\partial t}\left(\rho_m u_{m_i}\right) + \left[\left(\rho_m u_{m_j}\right)\frac{\partial u_{m_i}}{\partial x_j} - \sum_{\varphi=1}^{n}\left(\alpha_\varphi \rho_\varphi u_{dr_j\varphi}\right)\frac{\partial u_{dr_i\varphi}}{\partial x_j}\right] =$$
$$-\frac{\partial p}{\partial x_i} + \frac{\partial}{\partial x_j}\left[\mu_m\left(\frac{\partial u_{m_j}}{\partial x_i} + \frac{\partial u_{m_i}}{\partial x_j} - \frac{2}{3}\delta_{ij}\frac{\partial u_{m_i}}{\partial x_i}\right)\right] + \rho_m g_i, \tag{8}$$

$$u_{dr\varphi_i} = u_{\varphi_i} - u_{m_i}, \tag{9}$$

$$\mu_m = \sum_{\varphi=1}^{n} \alpha_\varphi \mu_\varphi. \quad (10)$$

There *i, j* are indexes of longitudinal and transverse flow directions; *dr* is a drift velocities index; *p* is a pressure, Pa; μ is a viscosity, Pa·s; δ_{ij} is a metric tensor.

For a non-stationary isothermal Manninen's multiphase conditions, the standard k-epsilon model [15] takes the form:

$$\frac{\partial}{\partial t}(\rho_m k) + \frac{\partial}{\partial x_i}(\rho_m k u_{m_i}) = \frac{\partial}{\partial x_j}\left[\left(\mu_m + \frac{\mu_t}{\sigma_k}\right)\frac{\partial k}{\partial x_j}\right] + G_k - \rho_m \varepsilon, \quad (11)$$

$$\frac{\partial}{\partial t}(\rho_m \varepsilon) + \frac{\partial}{\partial x_i}(\rho_m \varepsilon u_{m_i}) = \frac{\partial}{\partial x_j}\left[\left(\mu_m + \frac{\mu_t}{\sigma_\varepsilon}\right)\frac{\partial \varepsilon}{\partial x_j}\right] + C_{1\varepsilon} G_k - C_{2\varepsilon}\rho_m \frac{\varepsilon^2}{k}, \quad (12)$$

$$G_k = \mu_t S^2, \quad (13)$$

$$S = \left(2S_{ij}^{\ 2}\right)^{0.5}, \quad (14)$$

$$S_{ij} = \frac{1}{2}\left(\frac{\partial u_{m_j}}{\partial x_i} + \frac{\partial u_{m_i}}{\partial x_j}\right). \quad (15)$$

There *k* is a specific turbulent kinetic energy, J/kg; μ_t is a turbulent viscosity, Pa·s; ε is a specific turbulent kinetic energy dissipation, J/(kg·s); G_k is a turbulent kinetic energy generation due to the flow velocity gradient, J/(m^3·s); *S* is a viscous stress tensor modulus, 1/s; S_{ij} is a viscous stress tensor, 1/s. The values of the model constants were taken according to Launder's data [16, 17]: $C_{1\varepsilon} = 1.44$, $C_{2\varepsilon} = 1.92$, $\sigma_k = 1$, $\sigma_\varepsilon = 1.3$, $C_\mu = 0.09$.

Turbulent viscosity in accordance with [16] was determined by the Kolmogorov-Prandtl equation:

$$\mu_t = \rho_m C_\mu \frac{k^2}{\varepsilon}. \quad (16)$$

There $C_\mu = 0.09$ is a model constant [17].

The standard k-epsilon turbulence model [15] is an implicit model. Thus, this model makes it possible to simulate turbulent flows with relatively large discretization steps in coordinates and time, significantly exceeding the corresponding scales of turbulent vortices. In particular, the standard k-epsilon model allows to simulate turbulent flows even in a stationary setting. However, it is difficult to obtain accurate quantitative and spatial characteristics of turbulent vortices using the standard k-epsilon model.

Initially, for CFD simulation we planned to use 3D periodic meshes and models for explicit modeling of turbulent vortices, however, due to limited computing power at the time of works [12, 13], we had to abandon this idea. Even for accepted modeling techniques, the calculation time for each centrifuge operating mode was up to three weeks. The time discretizing step was no more than 10^{-5} seconds, otherwise the solution would crash. In addition, due to the joint use of the MRF and the relative velocities formulation, the physical time scale of the solution was distorted. When analyzing the simulation results, we could not talk about time in absolute units; instead, we used relative time, taking as a unit the duration of complete displacement of glycerol from the centrifuge rotor.

Despite the listed limitations, the results of experimental measurements and simulations of the glycerol concentration changes in the centrate during operation of the centrifuge for all considered modes differed by no more than 20-25% in the initial period of glycerol solution displacement and by no more than 10-15% in the final period [12].

Moreover, the experimental and modeling researchers' groups independently obtained similar data on a qualitative change in the hydrodynamics of the fluid in the centrifuge rotor in some operating modes. During the glycerol solution displacing, a change in the hydrodynamic regime from the conditional "laminar", characterized by a mixing length exceeding the axial extent of the centrifuge rotor, to the conditional "turbulent", characterized by large-scale axial and radial pulsations of the liquid phase was observed (Figure 3).

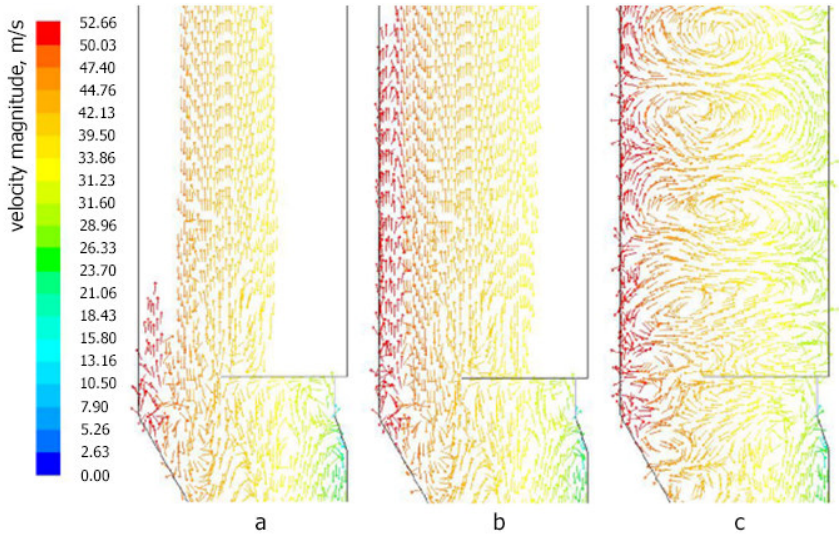

Fig. 3. Hydrodynamic regime changes: conditional "laminar" regime (a); start of the instability (b); conditional "turbulent" regime (c).

Thus, the following phenomena were established experimentally and computationally:

- the flow regime in the centrifuge rotor changes from conditional "laminar" to conditional "turbulent" in some operating modes;
- the changes in flow regime have no random nature;
- the amplitude of turbulent pulsations increases when the rotor rotation speed changes from 5000 to 6500 rpm and decreases slightly with a further increase in the rotor rotation speed.

Based on the results of observations and calculations, we assumed that the reason for the changing of the flow regime in the centrifuge rotor is resonance phenomena that occur when the rotor rotation frequency coincides with the natural frequencies of oscillations of the liquid flowing through the rotor. Understanding these phenomena is undoubtedly an important task, since changing the regime from the conditional "laminar" to the conditional "turbulent" can significantly reduce the solid phase particles sedimentation efficiency in the industrial centrifuge operating conditions. However, in the time of works [12, 13], research was not continued due to limited computational and experimental resources.

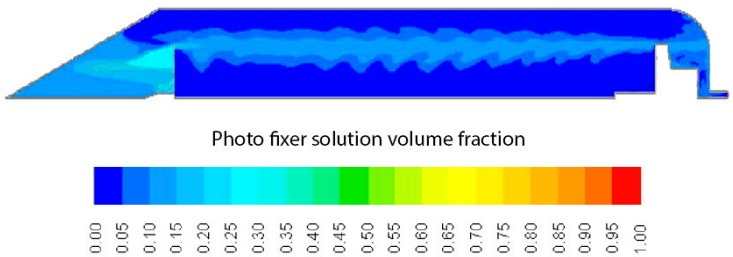

Fig. 4. Calculated scale of pulsations at the centrifuge rotor speed of 8000 rpm (rotated).

It should be noted that using numerical model with equations (4) – (16), the calculation of the velocity pulsations was essentially carried out almost directly, since the discretization steps, both in time and in space, corresponded to the scales of the pulsation rates (Figure 4). Apparently, only these conditions made it possible to simulate pulsation effects in principle.

Despite all the undeniable advantages of the standard k-epsilon model, this model was developed for purposes almost opposite to those set in our research. Therefore, the use of models that explicitly simulate turbulent phenomena is necessary in our case.

3 Numerical model and methods modernization

The increasing of available computing power has made it possible to make significant changes in mathematical models and methods for simulating the hydrodynamics of flows in the rotor of a high-speed centrifuge:

1. Instead of the axisymmetric 2D model, we were able to use the 5° angular extent sectoral 3D model and a structured prismatic mesh with a density of $4 \cdot 10^5$ elements.
2. Instead of the moving reference frame (MRF) method to set the rotor motion, we began to use the sliding mesh method [18], in which the motion is assigned directly to the mesh nodes.
3. The use of moving (sliding) meshes also made it possible to use an absolute formulation of velocities instead of a relative one.
4. Instead of the implicit k-epsilon model of turbulent pulsations, we began to use the LES-model (Large eddies simulation model) [19], which uses Smagorinsky approach with Boussinesq hypothesis [20, 21] for simulate large-scale eddies explicitly and small-scale (sub-grid) eddies implicitly.

LES-model uses this interpretation of Kolmogorov's theory:

$$u=u_{mean}+u_{pulsation}. \tag{17}$$

In the non-stationary formulation, all calculated velocities in Navier-Stokes equations are considered instantaneous (u). The eddy velocities corresponding to the mesh scale are calculated explicitly as mass-average velocities according to Kolmogorov (u_{mean}). Sub-grid-scale eddy velocities are calculated implicitly and correspond to Kolmogorov pulsation velocities ($u_{pulsation}$). The determination of pulsation (sub-grid-scale) and mass-average pressures (grid-scale) is like the determination of the corresponding velocities.

When using LES-model, the filtered by velocity and pressure Navier-Stokes equations are used. Filtering is carried out according to the following rule:

$$\overline{\theta}(x)=\int_D \theta(x')G(x,x')\mathrm{d}x', \tag{18}$$

$$G(x,x')=\begin{cases} V^{-1}, x'\in v \\ 0, x' \text{otherwise} \end{cases}, \tag{19}$$

There x and x' are grid-scale and sub-grid-scale coordinates; θ is a velocity, m/s, or pressure, Pa; D is a fluid domain, m^3; G is a filtering function; V is the volume of a grid cell, m^3; v is a volume, m^3; filtered variables are marked with a line at the top.

The conservation equations for mass and momentum in the Manninen's formulation, considering filtering, take the following form:

$$\frac{\partial \rho_m}{\partial t}+\left(\frac{\partial \rho_m \bar{u}_x}{\partial x}+\frac{\partial \rho_m \bar{u}_y}{\partial y}+\frac{\partial \rho_m \bar{u}_z}{\partial z}\right)=0, \tag{20}$$

$$\frac{\partial}{\partial t}\left(\rho_m \overline{u_{mi}}\right)+\left[\left(\rho_m \overline{u_{mj}}\right)\frac{\partial \overline{u_{mi}}}{\partial x_j}-\sum_{\varphi=1}^{n}\left(\alpha_\varphi \rho_\varphi \overline{u_{dr_j}}_\varphi\right)\frac{\partial \overline{u_{dr_i}}_\varphi}{\partial x_j}\right]=\frac{\partial \sigma_{ij}}{\partial x_j}-\frac{\partial \bar{p}}{\partial x_i}-\frac{\partial \tau_{ij}}{\partial x_j}, \tag{21}$$

$$\sigma_{ij}=\mu_m\left(\frac{\partial \overline{u_{mj}}}{\partial x_i}+\frac{\partial \overline{u_{mi}}}{\partial x_j}-\frac{2}{3}\delta_{ij}\frac{\partial \overline{u_{mi}}}{\partial x_i}\right), \tag{22}$$

$$\tau_{ij}=\rho\overline{u_i u_j}-\rho\overline{u}_i\overline{u}_j. \tag{23}$$

There σ_{ij} is a stress tensor due to molecular viscosity, Pa; τ_{ij} is a sub-grid stress, Pa.

As a result of the numerical model modernization, it was possible to increase the time step of the solution discretization from 10^{-5} to 10^{-3} s. The solution has remained stable, but it was decided to refuse a further increase in the time discretization step for the following reason. When limiting the maximum time step size for the solution, we proceeded from the

requirement that one revolution of the centrifuge rotor should not be less than 5–10 solution steps by the time.

The main result of the numerical model modernization, in addition to the solution stability increasing, is that the using the absolute formulation of velocities instead of the relative formulation makes it possible to accurately quantify not only the amplitude and step (length), but also the frequency of turbulent pulsations.

4 Results and discussion

Distributions of the velocities and volume fractions of glycerin and photo fixer solutions in the high-speed precipitation centrifuge rotor were obtained in the range of rotor angular velocity from 3,000 to 15,000 rpm using modernized numerical model. As a result of processing the simulation results, the dependences of the step, amplitude of pulsations and the frequency of vortex shedding from the centrifuge overflow disk on the rotor angular velocity were obtained (Figure 5).

The step and the amplitude of pulsations in the range of rotor angular velocities from 3,500 rpm to 6,000 rpm increase with slight acceleration and vary from 21.4 - 44.3 mm and 6.8 - 22.0 mm, respectively. In the range of rotor angular velocities from 6,500 rpm to 9,000 rpm the step and the amplitude of pulsations decrease with acceleration and take values from 31.4 - 12.8 mm and 26.3 - 13.2 mm, respectively. For the rotor angular velocities 9,000 rpm and above the decreasing of the step and the amplitude of pulsations decrease slows. The pulsations step here changes almost linearly and reaches the value of 8.6 mm at a rotor angular speed of 15,000 rpm. The pulsations amplitude at a rotor angular speed of 15,000 rpm reaches the value of 7.8 mm.

The form of the dependences of the pulsations step and pulsations amplitude on the angular rotor velocity suggests that at rotor angular velocity above 15,000 rpm, the pulsations step and amplitude values should reach saturation. However, calculations for such centrifuge operating modes have not been carried out. In addition, considering the frequency nature of resonance phenomena during centrifuge operation, the presence of a “second critical” rotor rotation speed (second resonant frequency) cannot be ruled out.

Figure 5 shows that the highest values of the step and amplitude of pulsations and the lowest values of the frequency of vortex shedding on the centrifuge overflow disk correspond to rotor angular velocity above 6,000 rpm and below 6,500 rpm. Thus, this angular velocity can be considered as a “critical” (resonant), since before it is reached, the amplitude (transverse pulsations) and the pulsation step (longitudinal pulsations) increase, and after its transition they decrease, which can be interpreted as a transition from a “subcritical” to a “supercritical” centrifuge operating mode.

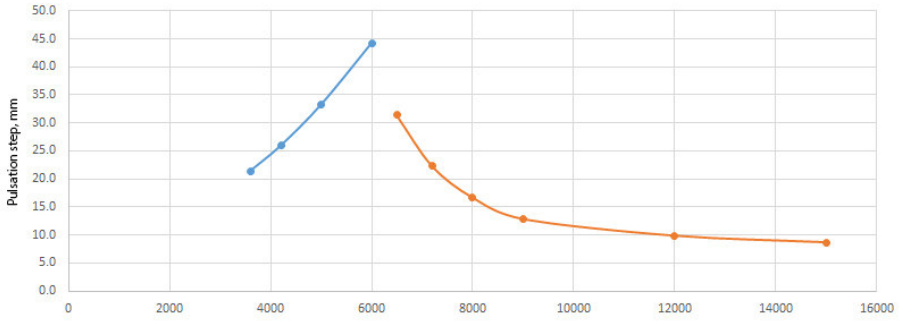

a)

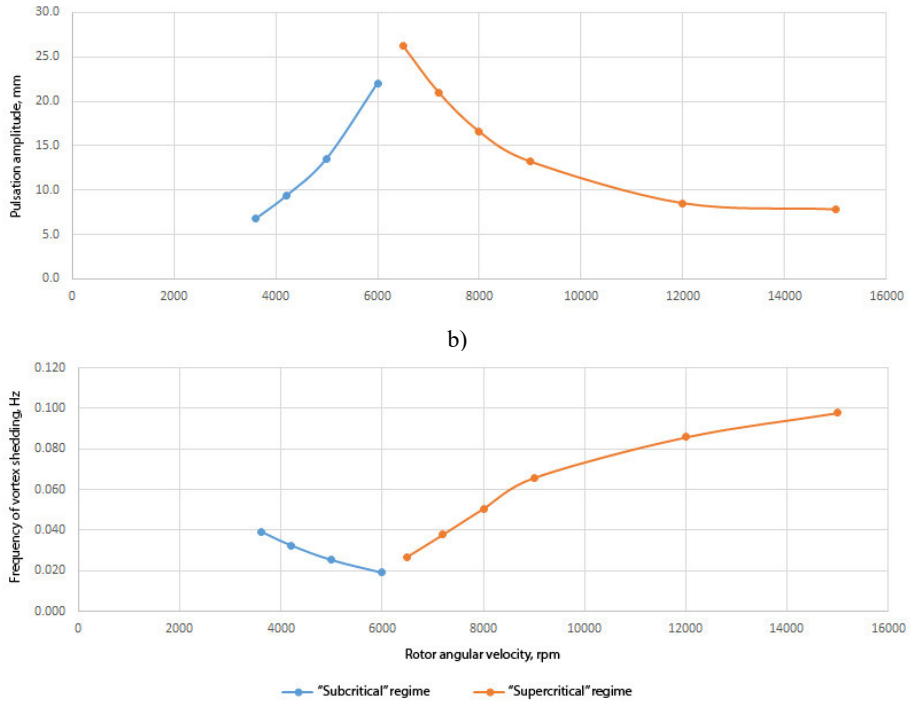

Fig. 5. Dependences of the pulsations step (a), pulsations amplitude (b), and frequency of vortex shedding from the centrifuge overflow disk (c) on the rotor angular velocity.

The calculated "critical" rotor angular velocity corresponds to a frequency of about 100-108 Hz for the mixture of glycerin and photo fixer solutions. The simulated frequencies of vortex shedding from the edge of the centrifuge overflow disk are in range of 0.019 – 0.098 Hz. That is, quantitatively, the frequency of forced oscillations (rotor rotation frequency) differs from the frequency of natural oscillations (vortex shedding frequency) by 4-5 orders of magnitude. Thus, it was not possible to establish a direct quantitative relationship between pulsation phenomena in the fluid flow through the centrifuge rotor and the rotor rotation frequency at this stage of our research.

It should be noted that the simulated frequencies of vortex shedding from the edge of the overflow disk in the entire considered range of angular velocities of the rotor are close to the calculated frequency of turbulent pulsations of the flow around the overflow disk, according to calculation from Strouhal number, the axial velocity of the flow and the thickness (length of the edge) of the overflow disk. The flow of the photo fixer solution in all considered cases remained constant and amounted to 40 l/h. At the same time, the frequency of vortex shedding from the edge of the overflow disk in the range of rotor angular velocities from 3,500 rpm to 6,000 rpm is reduced from 0.039 Hz to 0.019 Hz; in the range of rotor rotation speeds from 6,500 rpm to 15,000 rpm, the vortex shedding frequency increases from 0.027 Hz to 0.098 Hz. For the rotor rotation angular velocities above 9,000 rpm, the increase in vortex shedding frequency slows down.

Based on the results obtained, the main tasks of future research are:

1. better understanding of the physical nature of the instability of flows and the resonance phenomena in the rotor of a high-speed precipitation centrifuge;
2. oobtaining direct quantitative relationships between the forced oscillations frequency and the natural flow pulsation frequencies in the centrifuge rotor;

3. calculation of the resonant frequencies for liquids with densities and viscosities corresponding to the properties of real technological medias;
4. study of the influence of resonance phenomena in a centrifuge rotor on the behavior of solid phase particles of various sizes, shapes, and densities;
5. development of simpler, non-resource-intensive engineering methods for calculating resonance phenomena in high-speed centrifuges.

5 Conclusion

It has been shown experimentally and by the CFD simulation that during the operation of a high-speed settling centrifuge, two modes of liquid flow in the rotor are possible: conditional "laminar" and conditional "turbulent". The conditional "laminar" flow regime is characterized by a mixing path that exceeds the axial extent of the centrifuge rotor. The conditional "turbulent" flow regime is characterized by radial and axial pulsations, which lead to epy mixing intensification in the centrifuge rotor and to the solid particles' sedimentation efficiency reduction.

Using numerical simulation, it has been established that the flow pulsations are not random in nature. It is shown that the change in flow regime has a resonant nature, for which the frequency of forced oscillations is the rotor rotation frequency, and the frequency of natural oscillations is the frequency of turbulent pulsations in the fluid flow.

The numerical model and technic for simulating the hydrodynamics of a centrifuge rotor have been modernized. Instead of the implicit k-epsilon turbulence model, it is proposed to use the LES-model, which allows one to model grid-scale eddies explicitly, and sub-grid-scale eddies implicitly. In addition, instead of the method of moving reference frames (MRF), it is proposed to use the method of moving meshes, in which motion is assigned directly to the mesh nodes. The use of moving meshes made it possible to use an absolute formulation of velocities instead of a relative one. The use of the LES model makes it possible to give accurate quantitative estimates of the properties of flow pulsations, such as pitch, amplitude and frequency.

Using modernized numerical model, the dependences of the step, amplitude of pulsations and the frequency of vortex shedding from the centrifuge overflow disk on the rotor angular velocity were obtained in the range of rotor angular velocity from 3,000 to 15,000 rpm.

It is shows that the highest values of the step and amplitude of pulsations and the lowest values of the frequency of vortex shedding on the centrifuge overflow disk correspond to rotor angular velocity above 6,000 rpm and below 6,500 rpm. This angular velocity can be considered as a "critical" (resonant). The calculated "critical" rotor angular velocity corresponds to a frequency of about 100-108 Hz.

Based on the results of the research work performed, the tasks of future stages of the research were formulated.

In memory of Sergey Nikolaevich Syromyatnikov and Anatoly Ivanovich Snegin, our coworkers and teachers.

References

1. I.D. Wilson, *Encyclopedia of Separation Science* (Alfa Laval, Warminster, 2003)
2. M. Mory, *Fluid Mechanics for Chemical Engineering* (John Wiley & Sons, Inc, Hoboken, 2011)
3. N.A. Merentsov, N.S. Sokolov-Dobrev, A.V. Persidskiy, *Calculation of vibration resistance of a chemical reactor high-speed shaft undergoing torsional vibrations. Part*

I. Development of a block diagram and a dynamic transmission mode, in Proceedings of the 6th International Conference on Industrial Engineering, ICIE 2020, May 18–22 2020, Sochi, Russia (2020)

4. N.A. Merentsov, N.S. Sokolov-Dobrev, A.V. Persidskiy, *Calculation of vibration resistance of a chemical reactor high-speed shaft undergoing torsional vibrations. Part II. Defining model elastic-inertial parameters*, in Proceedings of the 6th International Conference on Industrial Engineering, ICIE 2020, May 18–22 2020, Sochi, Russia (2020)
5. N.A. Merentsov, N.S. Sokolov-Dobrev, A.V. Persidskiy, *Calculation of vibration resistance of a chemical reactor high-speed shaft undergoing torsional vibrations. Part III. Calculation of multi-mass system vibrations*, in Proceedings of the 6th International Conference on Industrial Engineering, ICIE 2020, May 18–22 2020, Sochi, Russia (2020)
6. R. Gueroult, J.M. Rax, N.J. Fisch, Phys. Plasmas **24** (2017)
7. Z. Hussain, S.J. Garret, S.O. Stephen, *Centrifugal instability over a rotating cone*, in 19th Australasian Fluid Mechanics Conference, 8-11 December 2014, Melbourne, Australia (2014)
8. Z. Hussain, S.J. Garrett, S.O. Stephen, P.T. Griffiths, Journal of Fluid Mechanics **788** (2016)
9. D. Zhilenko, O. Krivonosova, M. Gritsevich, IOP Conf. Series: Journal of Physics: Conf. Series **1163** (2019)
10. J.B. Flór, L. Hirschberg, B.H. Oostenrijk, G.J.F van Heijst, Physics of Fluids **30** (2018)
11. A. Aouidef, C. Normand, A. Stegner, J.E. Wesfreid, Physics of Fluids **6** (1994)
12. A.P. Khomyakov, S.V. Mordanov, V.A. Nikulin, S.N. Syromyatnikov, T.V. Khomyakova, A.I. Snegin, Proceedings of the Sverdlovsk Research Institute of Chemical Engineering. Series: technological production equipment **20**(**84**) (2012)
13. A.P. Khomyakov, S.V. Mordanov, V.A. Nikulin, S.N. Syromyatnikov, T.V. Khomyakova, A.I. Snegin, *Research of the fluid hydrodynamics in the rotor of a high-speed OVG-type centrifuge*, in Abstracts of the International Conference “70 years of SverdNIIhimmash”, 10-14 September 2012, Ekaterinburg, Russia (2012)
14. M. Manninen, V. Taivassalo, *On the mixture model for multiphase flow* (Technical Research Center of Finland, VTT Publications, Espoo, 1996)
15. B.C. Launder, D.B. Spalding, *Lectures in mathematical models of turbulence* (Academic press, London, 1972)
16. J.Y. Luo, R.I. Issa, A.D. Gosman, IChemE Symposium Series **136** (1994)
17. B.E. Launder, D.B. Spalding, Computer methods in applied mechanics and engineering **3**, 2 (1974)
18. G. Bachler, H. Schiffermüller, A. Bregant, *A parallel fully implicit sliding mesh method for industrial CFD applications*, in the Twelfth in an International meeting “Parallel computational fluid dynamics – trends and applications”, Parallel CFD 2000, 22-25 May, Trondheim, Norway (2000)
19. D. C. Wilox, *Turbulence modelling for CFD* (DCW Industries, San Diego, 2006)
20. J. Smagorinsky, Month. Wea. Rev. **91** (1963)
21. J. O. Hinze, *Turbulence* (McGraw-Hill Publishing Co., New York, 1975)